WINGBEAT MODULATION DETECTION OF HONEY BEES USING A CONTINUOUS WAVE LASER SYSTEM

by

Ryan Hall Scheppele

A professional paper submitted in partial fulfillment
of the requirements for the degree

of

Master of Science

in

Electrical Engineering

MONTANA STATE UNIVERSITY
Bozeman, Montana

July 2006

APPROVAL

of a professional paper submitted by

Ryan Hall Scheppele

This thesis has been read by each member of the thesis committee and has been found to be satisfactory regarding content, English usage, format, citations, bibliographic style and consistency, and is ready for submission to the Division of Graduate Education.

Dr. Joseph A. Shaw

Approved for the Department of Electrical and Computer Engineering

Dr. James Peterson

Approved for the Division of Graduate Education

Joseph Fedock

STATEMENT OF PERMISSION TO USE

In presenting this professional paper in partial fulfillment of the requirements for a master's degree at Montana State University, I agree that the Library shall make it available to borrowers under the rules of the Library.

I have indicated my intention to copyright this thesis by including a copyright notice page; as such, copying is allowable only for scholarly purposes, consistent with "fair use" as prescribed in the U.S. Copyright Law. Requests for permission for extended quotation from or reproduction of this thesis in whole or in parts may be granted only by the copyright holder.

Ryan Hall Scheppele

July 17, 2006

ACKNOWLEDGEMENTS

I would like to thank the following undergraduate research assistants that took part in this project for their diligence and enthusiasm: Amin Nehrir, David Hoffman, Charlie Keith, Jesse Way, Nick Jurich and Trent Jackson. This project would not have been possible without their help.

I would also like to thank Norm Williams for allowing use of the Physics Department Machine shop to create custom parts and also Christopher Melton who helped design the early versions of the Wingbeat Modulation Detector.

TABLE OF CONTENTS

LIST OF FIGURES

ABSTRACT

Using operant conditioning, researchers at the University of Montana have developed a technique for training entire colonies of honeybees to actively seek out explosive devices. The problem with this method of detecting explosives is that bees are difficult to track due to their small size. In an experiment in 2003, it was shown that a pulsed laser system could be used to detect bees; unfortunately this pulsed laser lacked the ability to resolve wingbeat modulation in the backscattered light.

This thesis describes the development of a monostatic, continuous-wave laser system capable of detecting modulation in backscattered light as a result of moving honeybee wings. Infrared light is generated by a laser diode and directed through a polarizing beam splitter and quarter-wave retardance plate which keeps the transmitted signal polarization perpendicular to that of the received signal. Using a photomultiplier tube as our detector, the backscattered light is converted into a current which is then sampled by an analog-to-digital device and stored on a computer. This stored data can later be processed using a sliding-window discrete Fourier Transform to determine the power spectral density with respect to frequency and time. By observing the power spectral density at the frequencies where honeybees are known to flap their wings (200 Hz to 250 Hz), our system can differentiate between light reflected by a honeybee and light reflected by stationary or slow-moving objects such as foliage.

CHAPTER ONE

INTRODUCTION

Demining

The U.S. State Department reports that landmines maim or kill nearly 10,000 people each year, though Landmine Monitor (2004) estimates that this number could be as high as 15,000 to 20,000 people each year. It is widely believed that as many as 50,000,000 unexploded ordnances (UXO) are scattered across 12,000,000 km² in as many as 100 countries across the world. Though global demining efforts have been making good progress over the last five years, MacDonald et al. (2003) predict that with current methods and rates, clearing the world of every existing landmine may not happen for another five centuries. Apart from being incredibly short-handed, current demining and area reduction rates are also limited by an overwhelming number of false positive landmine returns from conventional methods.

In response to the daunting task facing the demining effort, there have been numerous proposals for new detection methods that could potentially reduce the time needed to clear the world of landmines. Some of these techniques include electromagnetic induction (EMI), ground-penetrating radar, x-ray, acoustic/seismic and biological methods (such as dogs, bacteria, etc.) (MacDonald et al. 2003). Electromagnetic induction, for example, is a method that calls for little more than a metal detector, and has been in use since the First World War. This method is good for finding

landmines with an appreciable metal content, but is well known for reporting false positives when scrap metal or debris is buried in the ground. For instance, demining efforts in Cambodia between 1992 and 1998 recovered roughly 500,000 mines out of a total of more than 200 million potential hazards that were excavated from the ground (MacDonald et al. 2003).

Another approach is to use ground penetrating radar; unlike the EMI method, ground-penetrating radar has the ability to detect nonmetal landmines as well as metal ones. Ground penetrating radar was first used to detect landmines by the United States Army sometime in the 1940s, but has only become practical in the last few years (MacDonald et al. 2003). Ground penetrating radar is not too dissimilar from air-based radar: radio waves are transmitted into the ground, and reflections will be present anywhere an interface between the soil and other objects are present. Ideally, the ground penetrating radar would be used in an environment with perfectly homogenous soil, as any inhomogeneities in the soil will create reflections. The drawback to this approach is that naturally occurring features in the soil can look like landmines.

The acoustic/seismic methods calls for the use of lower frequency signals ($f < 1$ kHz) as a means of finding objects below the surface. Acoustic methods are less prone to false positive errors compared to EMI as this method does not depend on the metallic composition of landmines, and is apparently less susceptible to some of the obstacles that confound ground-based radar. Of course, the acoustic/seismic approach to locating landmines has a couple of limitations, the first being that sounds waves cannot travel far into the ground, ruling out the possibility of locating deeply buried mines or mines buried

in hard or frozen soil. In addition, the need for acoustic and seismic sensors to be very close to the ground will require a certain clearance from vegetation, which may not always exist.

All of the above described methods involve the use of electromagnetic radiation (or mechanical energy, in the case of acoustic/seismic detectors) to locate landmines. An interesting departure from the use of electromagnetic radiation involves methods based on detecting only the explosive chemicals themselves, with no regard to the container they are put in. One of the most well-known biological techniques is the use of mine detection dogs. Since the late 1970s, it has been known that dogs posses the capability to detect vapors from explosives in incredibly small concentrations. Phelan et al. (2002) determined that the chemical vapor sensitivity for 2.4-dinitrotoulene (2.4-DNT) in canines is on the order of 10^{-18} g/mL, but their results varied greatly at these low concentrations. Unfortunately, demining dogs can take up to a year to train; according to the Marshall Legacy Institute, the cost of "acquiring, training and delivering a certified mine detection dog to a contaminated country is approximately $20,000." In addition, demining dogs can take up to a year to properly train, and must be at least a year old to begin training. One final thing to consider is that dogs cannot detect landmines autonomously – they require a handler to lead them around the area under test, putting the human handler (as well as the dog) at risk of triggering a UXO.

One exciting development in the biological realm of demining was the discovery that *Apis mellifera*, a common species of honeybee, can smell 2.4-DNT. In fact, Bromenshenk et al. (2003) found that when properly conditioned to 2.4-DNT, honeybees

are capable of detecting vapor levels on the order of tens of parts per trillion (pptr) with low probability (less than 2%) of either a false positive or negative. Using a simple operant conditioning technique, an entire colony of honeybees can be trained in two days to actively seek anything emitting 2.4-DNT vapors; this is an incredible increase in training time over dogs. Moreover, with the exception of land near the Polar Regions, *Apis mellifera* can be found on every major continent, which eliminates the need for them to be trained in one location and subsequently shipped to another location as is the case with dogs (Bromenshenk et al., 2003). A further advantage of honeybees over canine detection is the fact that humans are needed only to condition and maintain the colonies; they are not needed to assist the bees in detecting landmines or other UXOs.

With proper conditioning, an entire colony of honeybees can be trained to act as nearly-ideal detectors of 2.4-DNT with vapor concentrations on the order of tens of pptr (Bromenshenk et al., 2003). By design, human interaction is required only to train the bees and not to detect a potential landmine or UXO, separating this method from many of those described earlier that put human beings at risk. One trial of this technique performed at Ft. Leonard Wood in 2003 (Shaw et al., 2005) showed that by observing the area under test and counting the number of bees found at a particular location, a conclusion can be drawn as to whether a UXO is at that location or not. The difficulty with bee-based demining is that observing bees is difficult beyond a few meters; this limitation applies to the human eye as well as sophisticated audio/video equipment. Thus, for bee-based demining to be practical, a system must be developed that has the ability to remotely detect bees at ranges on the order of tens of meters. A promising

approach to this problem is the design of an optical sensor that is capable of locating bees at ranges of tens to hundreds of meters.

An Overview of Optical Insect Detection

The first use of light as a means of detecting the beating wing of an insect can be traced back to Reed et al. (1941). In this paper, the authors were using the wingbeat frequency as a means of characterizing various species of *Drosophila*, or common flies. Here, the authors used a stroboscopic technique first used by Chadwick (1939), described as a "…neon-filled tube arranged in a tuned circuit so that the flash-frequency is instantly adjustable…" Each of the twenty-four specimens used in this experiment were glued to a paper strip and coerced into flying while inside the stroboscope apparatus. When the flash-frequency of the stroboscope is tuned to an integer multiple of the wingbeat frequency, the wings of the insect would be appear motionless to an observer.

Richards (1955) inadvertently discovered that a simple detector aimed at the sun was capable of detecting wingbeat modulation from insects flying in the solar path. In his setup, a cesium photoelectric cell was connected to an audio amplifier and loudspeaker and the signal was recorded onto magnetic tape. Over the course of his experiment, Richards observed "…occasional brief (< 0.25 sec.) random 'bursts' of sound occurred, of apparent frequency between 100 c./s. and 500 c./s." He concluded that these bursts were not caused by something visible to the naked eye. Later, Richards added another photoelectric cell and amplifier to his experiment, and found instances where a burst would appear on one channel and then on the second, separated by a certain

delay. Knowing the physical separation of the detectors and the inter-channel delay, he was able to determine whatever was causing these bursts had a velocity of roughly 5 to 10 miles per hour; later, he concluded with certainty that these signals were caused by insects.

The next major step in optical insect detection was Unwin and Ellington (1979) and the optical tachometer. Using an AC-coupled photodiode followed by a two-stage amplifier with a high-pass response, the authors were able to detect wingbeat modulation from only the ambient light in the room, created by DC-driven lamps or daylight. Unwin and Ellington noted that the use of "…artificial lighting powered from an alternating supply results in so large an output at 100 Hz that the signal is masked completely." Depending on the size of the insect, the optical tachometer could be operated at a range of 1-10 meters indoors. Moore et al. (1986) used this optical tachometer as a means of finding the wingbeat frequencies of various insects with the intent of creating a system that could automatically identify insects based on these frequencies, with two major differences. The first difference was that Moore et al. digitized the signal for storage on a personal computer. The second difference was that Moore observed the harmonic content of the insect signals as well as the fundamental wingbeat frequency. This work eventually evolved into OFIDIS (Optical Flying Insect Detection and Identification System) (Moore, 2001).

Each of the optical insect detection methods listed are effective in that they can resolve the beating wing of an insect; however, each method listed requires that the insect fly between a light source and a detector. This is quite inconvenient with regards to

demining, as this constraint precludes any sort of scanning motion without moving the light source (or detector), which may be difficult near an area littered with landmines or other UXOs. In addition, this requires that both the source and detector must be located in accessible areas; it is easy enough to imagine a case where line-of-sight cannot be established across a mined area between the source and detector. For an optical detection system to be practical for demining, it should be able to function without this constraint. The solution to this problem is to use an optical detection system based on backscattered light, which allows for the possibility of the source and the detector being placed very close to each other. The obvious solution to this problem is to use a LIDAR (Light Detection and Ranging) instrument as a means of detecting bees.

LIDAR-based Insect Detection

In 2002, a team of researchers from Sandia National Laboratory determined that honeybees could be detected by a horizontally-pointed, 355 nm LIDAR (Bender et al., 2003). In their experiment, the LIDAR was pointed above a feeder at a distance of over one kilometer; by observing the backscattered light, they concluded that they could detect bees hovering over the feeder. While data obtained from a LIDAR can be manipulated to determine the range to a target using a time-of-flight calculation, a fixed LIDAR is incapable of detecting anything other than what lies in the field of view (FOV) of the instrument. Still, this experiment demonstrated the viability of a laser-based detection system.

The following year, a blind field trial was conducted at Ft. Leonard Wood in Missouri by researchers from the University of Montana (UM) and Montana State University (MSU) and the National Oceanic and Atmospheric Administration (NOAA). During this trial, which took place from July 25th to August 5th, 2003, honeybees conditioned by the UM team flew over an area 24 m wide and 44 m long while a Nd:YAG-based LIDAR developed by NOAA and located 83 m away was scanned across the field at a rate of 1.46 degrees per second (Shaw et al., 2005). By keeping track of the angle of the outgoing beam with respect to the field, the team from MSU was able to generate a map of bee densities across the field over a certain period of time creating a bee-density histogram as a function of angle and range. This map was then used to link areas of high bee density with vapor plumes from the unexploded ordnances located in the area. Shaw et al. found that the scanning LIDAR did detect a higher density of bees in the locations where 2.4-DNT vapor plumes were present, but when the LIDAR-generated map was compared to the chemical plume map, the correlation coefficient between the two maps was 0.38. Shaw hypothesized that one of the reasons for this was that the LIDAR could only be scanned 60 cm up from the ground level before vegetation became visible in the backscattered light, allowing room for the honeybees to fly under the laser beam. Even after mowing the field and lowering the height of the LIDAR, honeybees could still be observed flying under the beam, suggesting that a "bee-specific detection mechanism is needed so that the laser beam can be swept closer to the ground and so that bees can be detected as they fly through the vegetation" (Shaw et al., 2005).

Clearly, a laser-based system utilizing backscattered light seems like a reasonable approach for detecting honeybees across an area potentially littered with landmines, but the experiment at Ft. Leonard Wood demonstrated that a simple LIDAR will not be able to distinguish between a honeybee and fixed targets such as vegetation. Our proposed method calls for a continuous-wave (cw) laser system that detects backscattered light. This technique will have the advantage of being able to detect modulation in the backscattered light created by the moving wings. Using spectral analysis and knowledge of the wingbeat frequency of a honeybee, we will be able to differentiate between light reflected by stationary or slow-moving targets like vegetation and light reflected by honeybees. Although the cw system is not capable of directly measuring range, it allows a simple and compact sensor system that may be useful in applications such as area reduction (determining which areas have mines and which do not). An alternate approach is to co-scan two cw instruments and use triangulation to determine bee locations.

CHAPTER TWO

SYSTEM DESCRIPTION

Optical Configuration

The Wingbeat Modulation Detector (WMD) is essentially a monostatic LIDAR that uses a continuous-wave laser in place of a pulsed laser. Infrared light is generated by a JDS Uniphase laser diode operating at a wavelength of 808 nm. The decision to operate at this wavelength is balanced between two main factors: detector availability and invisibility to humans. To maximize the sensitivity of the detection portion of this instrument, a photomultiplier tube was chosen as the detector. Unfortunately, the radiant sensitivity of photomultiplier tubes does not extend very far into the infrared region, forcing the use of a near-infrared laser for this system. Ideally, a shorter wavelength just outside of the visible range would yield better radiant sensitivity from the PMT, but the 808 nm diodes were on hand at the time this system was being built. Other benefits to keeping the laser beam invisible is the possibility of semi-covert UXO detection and lower solar background relative to the background at visible wavelengths. In addition to the infrared laser, a green laser has been integrated into the WMD to provide a visual indication of the field of illumination.

Light leaving the laser diode has an elliptical cross-section, due to the shape of the gain region in the diode itself. An anamorphic prism pair is placed directly after the diode to produce a more circular beam; our prism pair is placed backwards to create a larger diameter circular beam. The infrared light is steered by two dielectric mirrors

through a dichroic mirror and onto a positive lens with a focal length of 50 mm. The beam then bounces off the interface inside the polarizing beam splitter, through a quarter-wave plate, through the primary lens (focal length of 450 mm) and finally reflects off of the scanning mirror seen in the lower-right corner of Figure 1. In the first prototype, this scanning mirror was a simple bathroom mirror tile attached to a Zaber Technologies stepper motor using a custom-built mount. This mirror is by no means ideal, as it is not a front-surface mirror, but it worked well enough to demonstrate the basic feasibility of the technique.

Figure 1. Block diagram of the Wingbeat Modulation Detector.

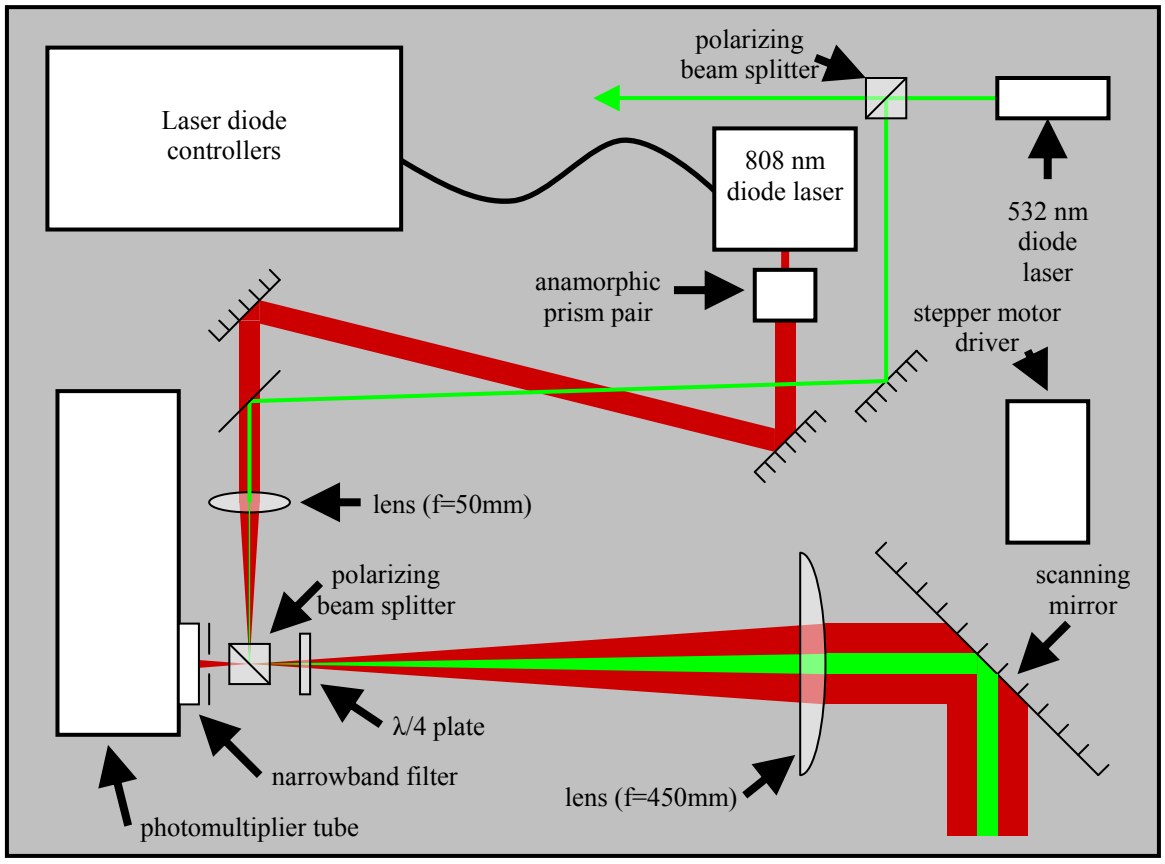

Since the polarization purity of the laser diode is on the order of 500:1, only a small percentage of light is lost as the beam hits the polarizing beam splitter and leaves the system. Also, the ratio of the focal lengths of the Keplerian telescope formed by the two positive lenses gives a beam expansion factor of 9. Expanding the beam reduces the irradiance of the beam at the target, but should increase the probability of catching a honeybee in the beam.

Figure 2. Photo of the Wingbeat Modulation Detector *(photo by Joseph A. Shaw)*.

After reflecting off of a target, the circularly polarized light will change directions: for example, counter-clockwise circular light would become clockwise circularly polarized. Light that gets back into the system will be transformed back into

linearly polarized light by the quarter-wave plate; only the light will now be oriented 90° from its original axis. This backscattered light now passes straight through the polarizing beam splitter, through a narrowband optical filter and is focused onto the active area of the photomultiplier tube. The narrowband filter was manufactured by CVI Laser and has a full width half max (FWHM) transmission rating of 10 nm. The purpose of this filter is to reduce the amount of background light not originating from our instrument from getting onto the active area of the detector. Realistically, the bandwidth of the optical filter is orders of magnitude wider than the linewidth of the diode laser which means that a fair amount of scattered solar radiance in this band will end up in the PMT. By limiting the field-of-view of the detector to the field-of-illumination of the transmitted beam, the amount of background optical power entering the detector can be reduced, but background light is nevertheless a factor that limits this sensor's sensitivity to wingbeat signals. The PMT used in this system is a Hamamatsu R3896 which is designed for use in the visible range, yet has marginal quantum efficiency and radiant sensitivity in the near-infrared range. At 808 nm, for example, the R3896 has a quantum efficiency of 6-7%, and radiant sensitivity of 50 mA/W, compared with its peak quantum efficiency of 90% and 90 mA/W at 450 nm.

The largest annoyance with the monostatic configuration is the relatively high number of components required to make the system work. One problem with the high component count is the optical power lost in each element. In this sensor, the infrared laser beam must be transmitted or reflected by nine components; the received beam is affected by only five. To a small degree, this effect can be reduced by using more laser

power than would be used with a simpler bistatic setup. The laser diode used in this instrument has a maximum output power of roughly 100 mW, which is enough power to demonstrate system functionality indoors: however, this may not be enough optical power for this instrument to work well outside, a topic that is explored in more detail later in this paper.

The other problem inherent to this design is that keeping the field of view (FOV) and field of illumination (FOI) aligned over a large distance is egregiously difficult due to the number of components that must be properly positioned to keep the FOV and FOI coaxial. In addition, the back reflections from the quarter-wave plate and the positive lens must be taken into consideration. Initially, these components were aligned under the assumption that they should be perfectly normal to the optical axis. The problem we ran into was that the back reflections were bouncing straight into the PMT, bringing us closer to saturating the detector and forcing us to use a lower supply voltage. Fortunately, this mistake was caught early in the development of this system, and was corrected. The longer-term solution is to use anti-reflection-coated optical components.

Figure 3. Geometric comparison of monostatic and bistatic configurations.

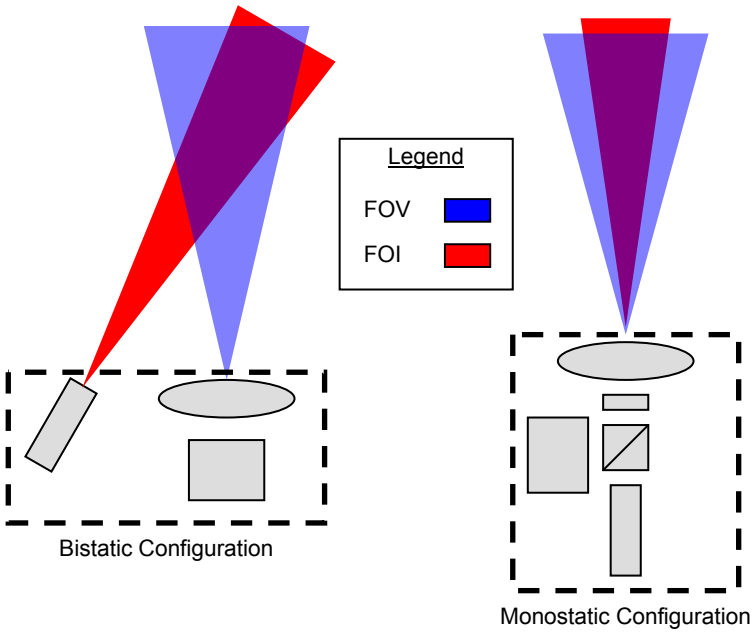

Assuming proper alignment, the monostatic configuration has a slight advantage over its bistatic counterpart in that the field of view (FOV) of the detector and the field of illumination (FOI) of the laser are ideally coaxial in a monostatic system; this advantage can be seen in Figure 3. The right half of Figure 3 shows a typical monostatic configuration and the left side a bistatic configuration; please note that the proportions in this figure are exaggerated to better illustrate differences between the two approaches to backscatter-type laser instruments.

Alignment

After building the system, a method had to be devised to ensure that the FOV/FOI were, in fact, coaxial to each other. Finding the FOI is as simple as turning the laser on and viewing the laser spot through an infrared viewer, but this does nothing for finding the FOV. Early attempts at using a mirror to reflect the infrared light back into the receiving optics worked well with the absence of lenses, and at short distances, but once these optics were replaced this technique proved less than useful.

After much deliberation, it became evident that the only way to find the FOV would be to use another infrared light source at a certain distance away from the WMD. In this case, the light source used was a simple infrared light-emitting diode (LED) connected to a DC power supply. While observing the signal out of the photomultiplier tube, the infrared LED was moved in a raster fashion to determine the boundaries of the FOV. Using a large poster board, the edges of the FOV could be approximated, and the FOI traced while using an infrared viewing scope. By repeating this test over a series of distances, it was believed that we could see the trend in the position of the laser spot with respect to the FOV and take the appropriate action.

After doing this experiment at several distances, it became clear that the laser beam was indeed inside the FOV for shorter distances (< 8 m) but began moving out of the FOV beyond that. Correcting this required a few iterations of adjusting mirrors and re-checking the FOI and FOV at multiple ranges; ultimately, we were able to keep the FOI and FOV coincident for roughly 30 m, which is coincidentally the length of the longest indoor hallway available to perform this experiment.

Electronics

A Stanford Research Systems preamplifier (model # SR560) was used in this system to condition the electrical signal leaving the photomultiplier tube. The SR560 has several useful features that make it very desirable for this laser system: multiple coupling options, built-in filter banks, adjustable gain and the option to run on batteries.

Figure 4. The Stanford Research System SR560 Preamplifier.

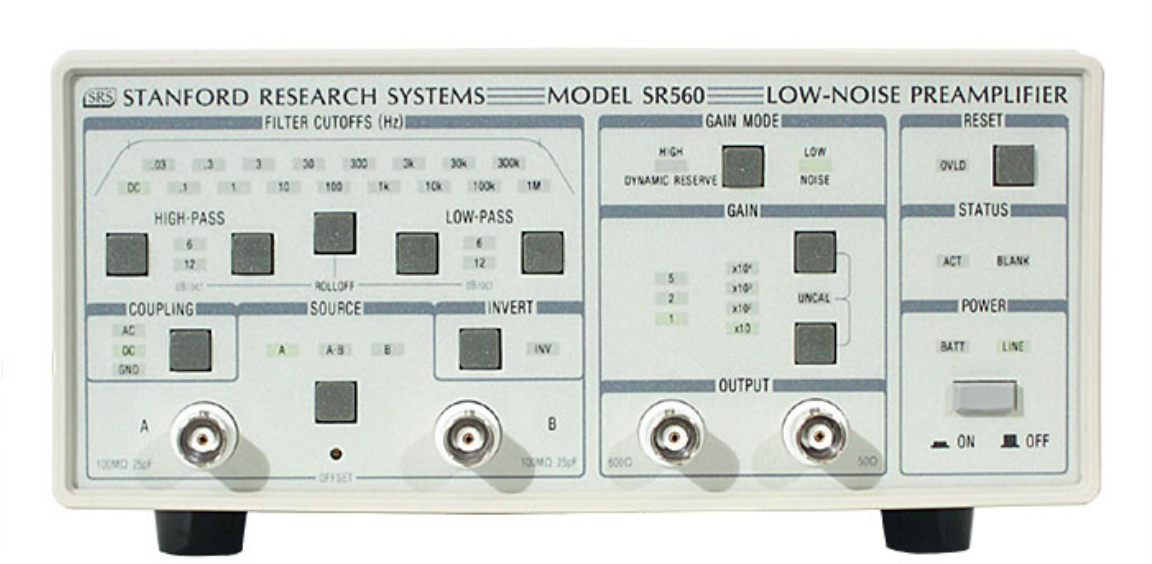

The built-in filters of the SR560 were setup in the bandpass configuration with the lower cutoff frequency at 30 Hz and the higher cutoff frequency at 1 kHz. The purpose of these filters is purely to limit the bandwidth of the signal being sent to the analog-to-digital card; a typical constraint of discrete sampling theory that prevents the inclusion of higher frequency signals in the sampled data through aliasing. In our case, the sampling

rate of the analog-to-digital (A/D) converter card was set to 5 kHz; according to sampling theory, we need only sample at a rate which is at least two times the frequency of the fastest signal found in the analog stream. Since the high corner of the bandpass filter is set to 1 kHz, a minimum sampling frequency of 2 kHz is needed in order to properly prevent aliasing in the reconstructed signal with an ideal filter; sampling at higher frequencies serves as a way to reduce the amount of noise present in the digitized signal.

The input coupling options of the SR560 allow us to AC-couple the signal from the PMT before it is filtered and amplified. This is convenient in that the signal from the PMT has a tendency to slowly 'wander' as the mirror is scanned across an area under test. This slow 'wander' is due to changes in the reflectivity of the background illuminated by the infrared laser light. After AC-coupling and bandpass filtering the PMT signal, it is then amplified by a factor of 1000 V/V (60 dB) and sent into the A/D converter. This high gain factor is necessary because the output range of the PMT is on the order of millivolts; without amplification, the signals we are trying to detect would be on the same order of magnitude as the sampling noise of the A/D converter.

The A/D converter used in the wingbeat modulation detector is a National Instruments model PCI6220. This A/D card has a maximum sample rate of 200 kS/sec at a sampling resolution of 16 bits over a voltage range of ± 1 V yielding a resolution of 360 μV. The card has a PCI interface with a full driver suite written by National Instruments as part of the LabView software which makes control of the A/D card and storage of the sampled data very straightforward.

Figure 5. I/O block for the A/D card and computer.

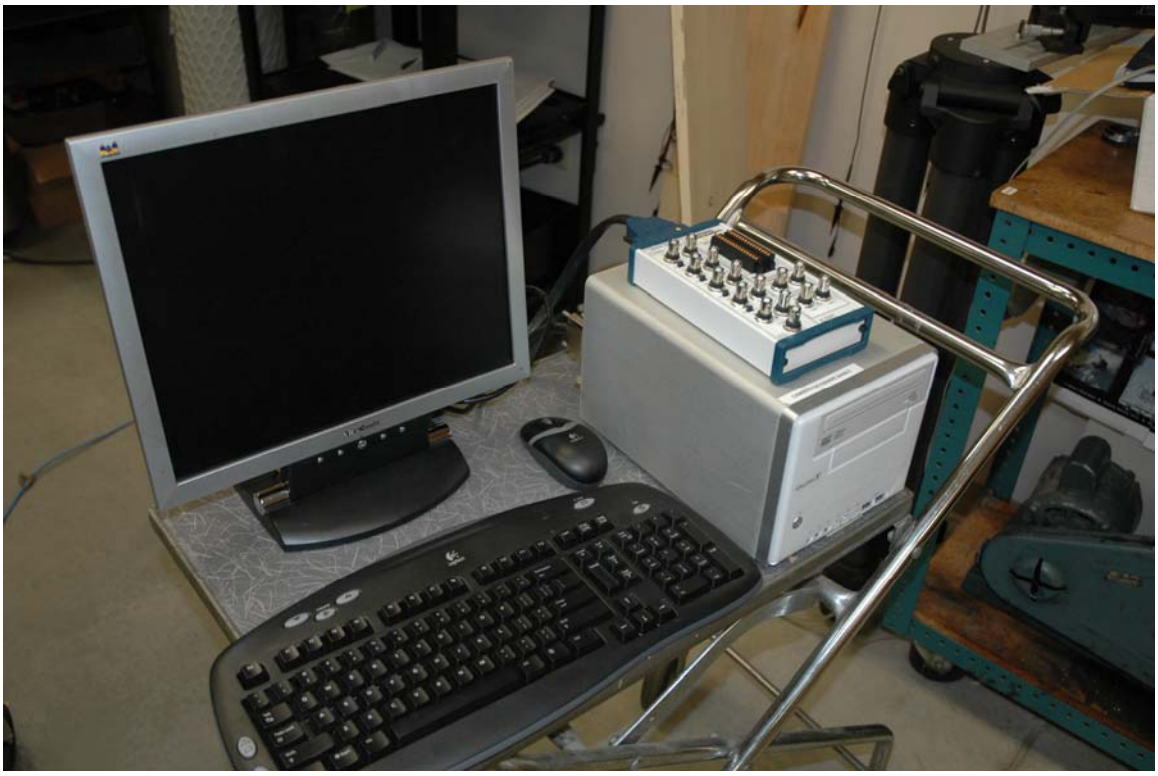

The computer built to house the A/D card is based on a Shuttle barebones system, which was populated with a processor, memory, an optical drive and a hard drive. In particular, this system was designed to be powerful enough to run the necessary software without the need for a full-size desktop case. Apart from the small form factor of the case itself, however, there is nothing out of the ordinary about this computer.

Software

Data Acquisition

Storage of the sampled data from the Wingbeat Modulation Detector is handled by a program written in the National Instruments LabView suite; this program also controls the Zaber Technologies stepper motor that drives the turning mirror. As with all LabView programs, this program is separated into two distinct pieces: the front panel, which serves as a user interface to the block diagram, which houses the "code" of the program.

The front panel for the WMD control program (Figure 6) is designed so that the user can see the sampled signal in several different forms to make the data easier to interpret. In the upper left-hand corner, a one second chunk of data is plotted in simple x-y fashion. In the upper right corner appears a power spectral density (PSD) plot of the data being displayed since this system is designed to detect modulation of backscattered light. To make trends in the PSD easier to identify, successive frames of the PSD are concatenated and displayed, forming a spectrogram which appears in the lower-left corner of the window. To the right of the spectrogram appear the stepper motor controls, laser parameter settings, and the "Go!" button, which runs the program.

Figure 6. Front panel for the data acquisition program.

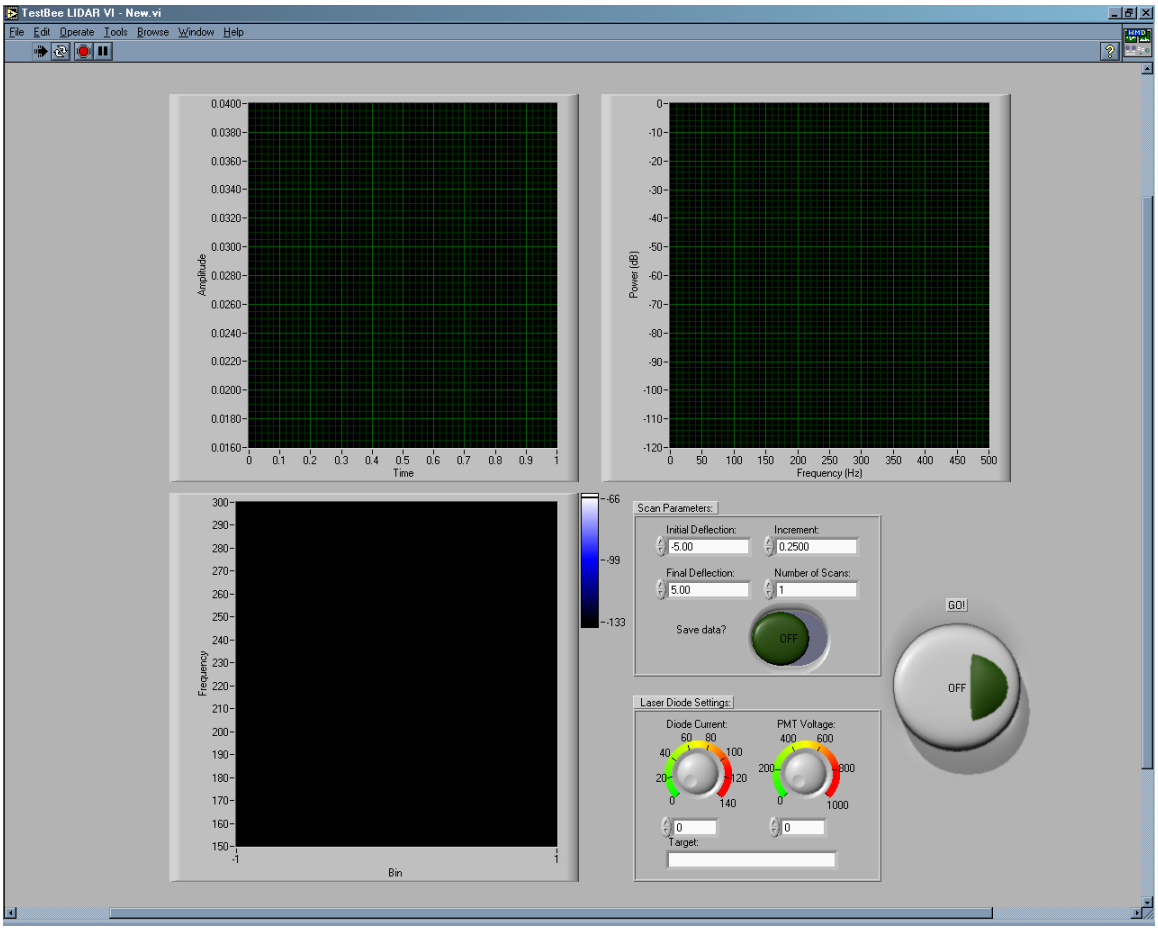

The block diagram of the WMD control program performs three main functions: setting up the file/folder structure for the sampled data, initializing the stepper motor and collecting and saving the sampled data. Unlike a traditional programming language, in which software is written line-by-line, a LabView program is comprised of icons, representing functions and subroutines, with connections running between them. This approach tends to simplify the task of writing a program, yet larger programs can become very hard to understand, as they may grow so large that they can only be viewed in

pieces; such is the case with the block diagram for the WMD control program. As such, inclusion of any images of this block diagram would be difficult to include without a loss of readability in a paper.

The file/folder structure generated in the block diagram allows data to be separated into folders based on the date and time of each test, as well as allowing for the laser parameters to be written into the lowest-level folder. Sampled data are saved into one-second chunks from each angular position of the scanning mirror; angular information is embedded into the file name, as is the scan number, in the case of a test involving multiple scans of the mirror.

Communication with the stepper motor is achieved using functions written in LabView by Zaber Technologies that utilize the serial port of the computer. After setting the mode of operation for the stepper motor, the drive current and hold current settings are sent to the motor controller. Next, the position buffer in the controller is reset to a known value and then moved to the initial position for the scan. Once the mirror has stopped moving, the program will collect data for one second and then move to the next position until the scan is complete.

Signal Processing

The signal processing routines designed to interpret sampled data from the WMD are written exclusively for the Mathworks program Matlab; the availability of myriad pre-existing functions and programs being the largest reason for choosing this suite. Upon execution, the user is prompted with a dialog box to browse for a folder containing the information to be processed. Once a valid folder has been chosen, all of the files in

the folder are loaded into the Matlab workspace. Since we are interested in detecting modulation at a particular frequency at a given moment in time, the power spectral density (PSD) must be found for each data set from the different angle bins. The most convenient way of doing this is to use the `spectrogram()` function in Matlab, which performs a sliding-window Discrete Fourier Transform (DFT) on the sampled data. The result of the spectrogram is a two-dimensional matrix that gives the power spectrum as a function of time. A typical spectrogram is shown in Figure 7. This spectrogram is of a frequency-chirped signal generated by a function generator and sampled by the A/D card.

Figure 7. A spectrogram showing a frequency-chirped signal.

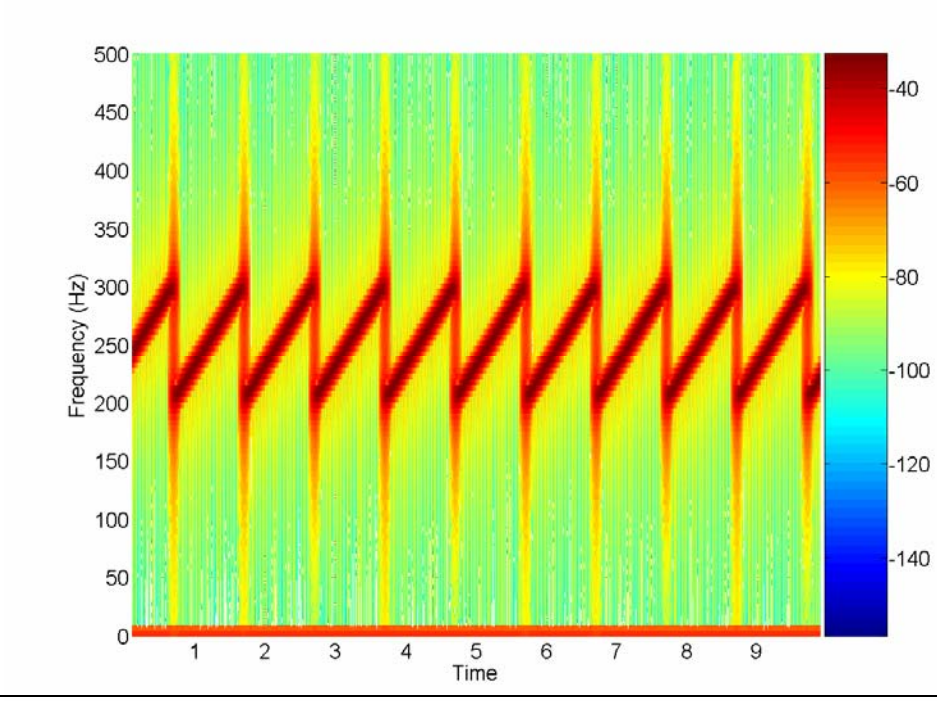

Once the time-dependent PSD has been found for each angle bin, each of these two-dimensional matrices is concatenated to create a composite 2-D matrix that

represents the power spectrum as a function of angle bin. Once this composite matrix has been formed, it can be viewed using the *image()* command; after scaling and labeling the axes, the resulting image resembles Figure 8. The importance of this particular spectrogram will be explained later; for the time being assume that the reddish bursts around 150, 300 and 450 Hz and located horizontally near the middle of the spectrogram represent modulation produced by a honeybee.

A large annoyance to the image in Figure 8 is the presence of 60 Hz line noise in the sampled data, along with the presence of harmonics. In addition, the presence of a strong DC component in the return signal tends to dominate all other components of the signal, meaning that the resulting image will be scaled in a manner largely unfit for identifying short bursts of modulation, as would be expected from a honeybee. To combat this, a method was devised for removing components of the return signal that were static with respect to time, that is, signals appearing as horizontal lines in a spectrogram-type display. To do this, a median was performed on the composite PSD matrix to find the median value of the PSD with respect to time. The median PSD values for the frequencies of interest are then subtracted from each 'slice' of the composite PSD, resulting in a power spectrum without the presence of line noise or DC, as in Figure 9.

Figure 8. Composite PSD matrix displayed in Matlab.

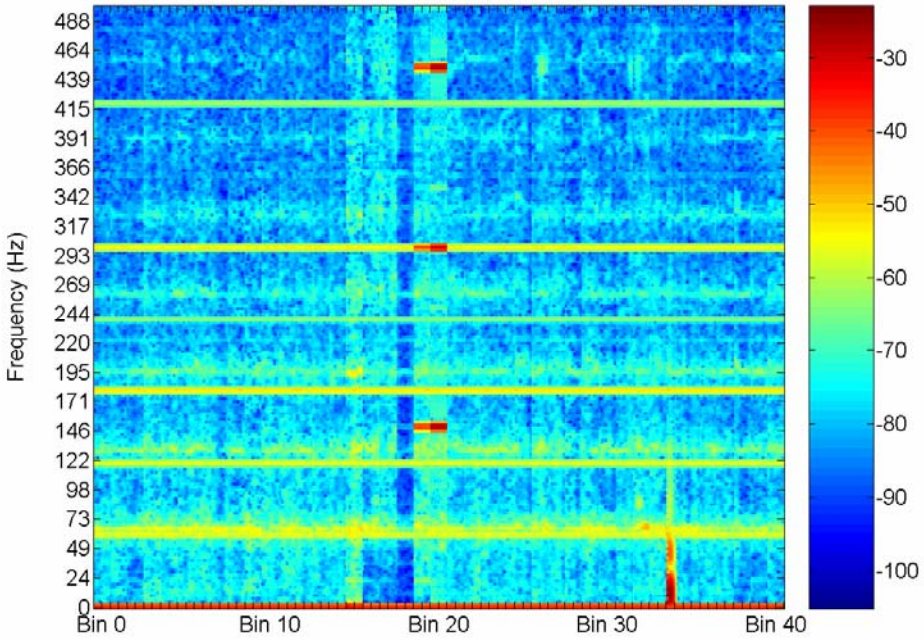

Figure 9. Composite PSD with median subtraction.

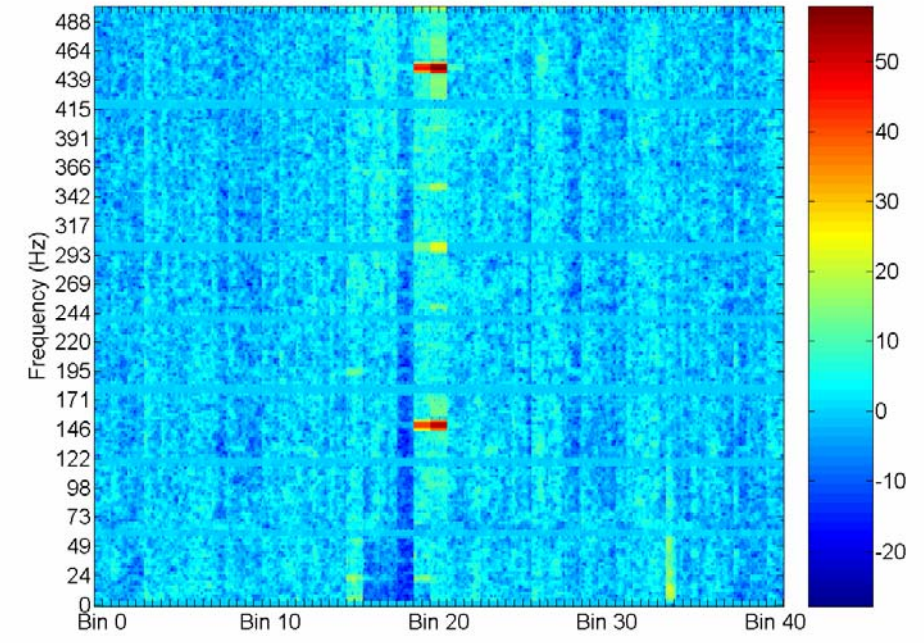

This ‘median subtraction’ operation, it seems, has done a reasonably good job of removing the 60 Hz line noise as well as the large DC component. While the simulated bee return near bin 20 now stands out more, the image is still fairly noisy, which may present problems for a processing routine designed to identify bursts of modulation. One way to handle this noise is to apply nonlinear scaling to the image to increase the contrast between a bee return and the noisy background. In addition, this scaling can smooth out the noisy background, which makes the use of a first-difference type filter for identifying features practical.

Figure 10. Median-subtracted composite PSD with map scaling.

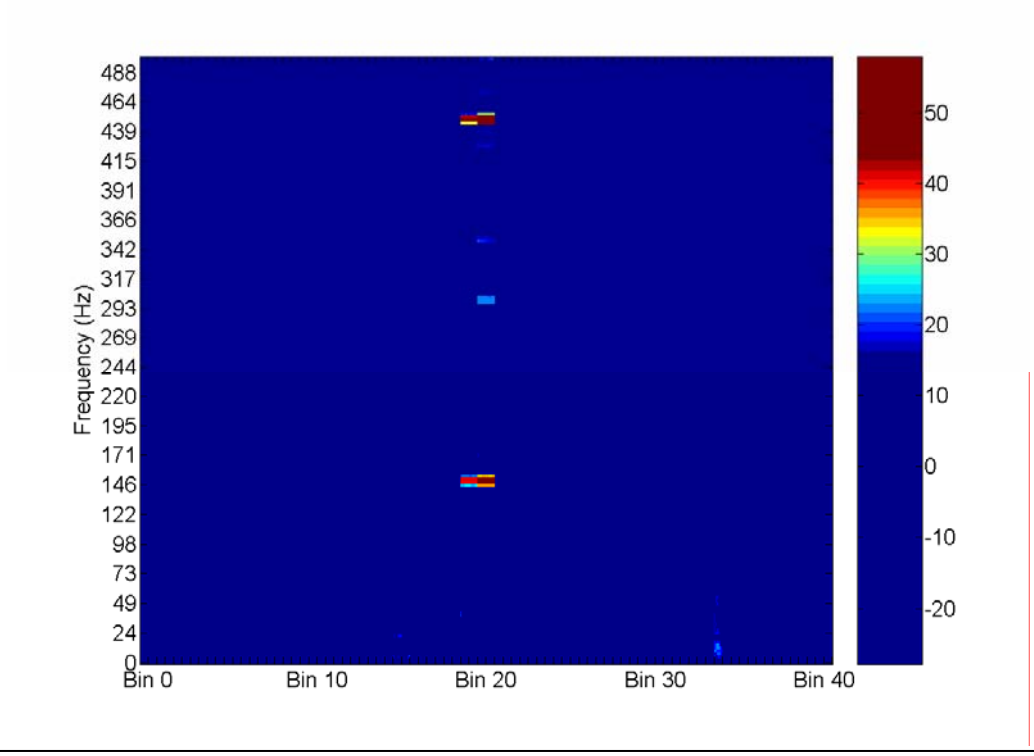

In Figure 10, the colormap has been rescaled, creating an image that is many times simpler than Figures 8 and 9. To accomplish this rescaling, the original colormap

has been compressed, shifted and padded; this establishes a threshold which will be used to differentiate a genuine bee return from noise. The caveat to this approach is that the map scaling must be finely tuned; the lower the threshold, the greater the chance of a false positive, and vice versa.

CHAPTER THREE

EXPERIMENTAL DATA

With the field of illumination (FOI) and field of view (FOV) properly aligned, the next step in the testing of the Wingbeat Modulation Detector (WMD) is verifying the ability of the instrument to detect modulation in the backscattered light as a result of the beating wings of a honeybee. In the early stages of this project, attempts were made to catch honeybees and bring them into the laboratory; by placing them in small containers, we could easily fire the laser on the honeybee itself. Unfortunately, these experiments failed because the bees simply would not fly once placed in a small container.

With live bees ruled out, we needed to find a controlled method of simulating the effect that a moving bee wing would have on the backscattered light. The idea of using a chopper wheel was proposed and tested; using a chopper wheel works, but does not emulate the motion of a bee wing well enough to provide reliable data.

It was no small stroke of fortune that one of the groups in the Physics Department at Montana State University, led by V. Hugo Schmidt, has been developing a piezo-electric polymer (PEP) for use in microgravity vibration isolation applications (Bohannon et al., 2003). The sample we received was comprised of two sheets of PEP bonded together; applying a large sinusoidal voltage across this composite PEP sheet caused the sheet to move back and forth at the frequency of the sinusoid. At first, we were only able to drive the sample at tens of Hz, but after cutting the PEP to the same size as a bee wing, we were able to make the PEP flap at a frequency of 150 Hz.

Figure 11. The piezo-electric polymer *(photo by Joseph A. Shaw)*.

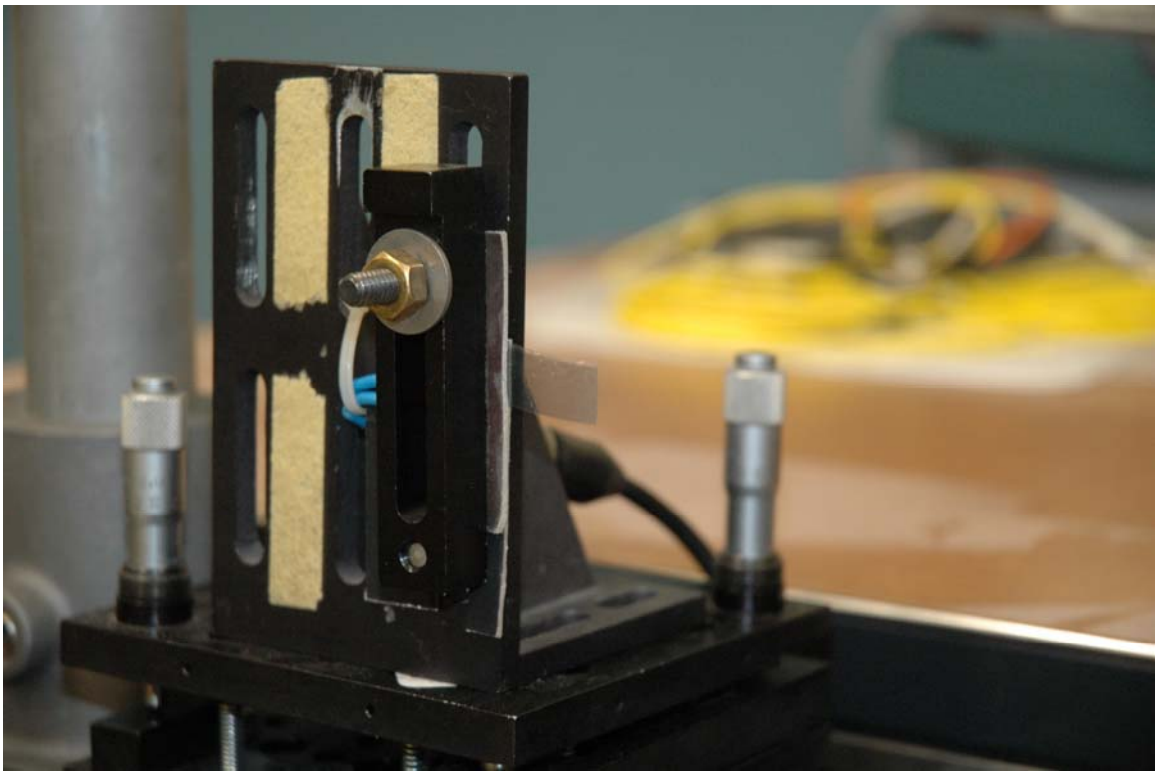

After mounting the PEP and running several experiments (Figure 11), it became clear that the WMD was indeed quite capable of detecting modulation in the backscattered light as the result of a moving target. Figures 8, 9 and 10 all show data from an experiment where the WMD was set to scan an area that included the PEP. With these results, the next step was to take the instrument outside and try to detect honeybees. Before this step can be taken, however, it may be prudent to develop a working model of this instrument to ensure that the current configuration of the system will yield acceptable performance outdoors.

CHAPTER FOUR

MODELING

To describe the performance of the Wingbeat Modulation Detector (WMD), we begin with the radiometric model describing the light transmitted by the WMD and how it interacts with the target. We assume a laser beam with an initial radius r_0 and a divergence half-angle θ_{DIV}, as well as a distance z separating the transmitting lens and the target. The graphical interpretation of this model is shown in Figure 12:

Figure 12. Radiometric model of the Wingbeat Modulation Detector transmitter.

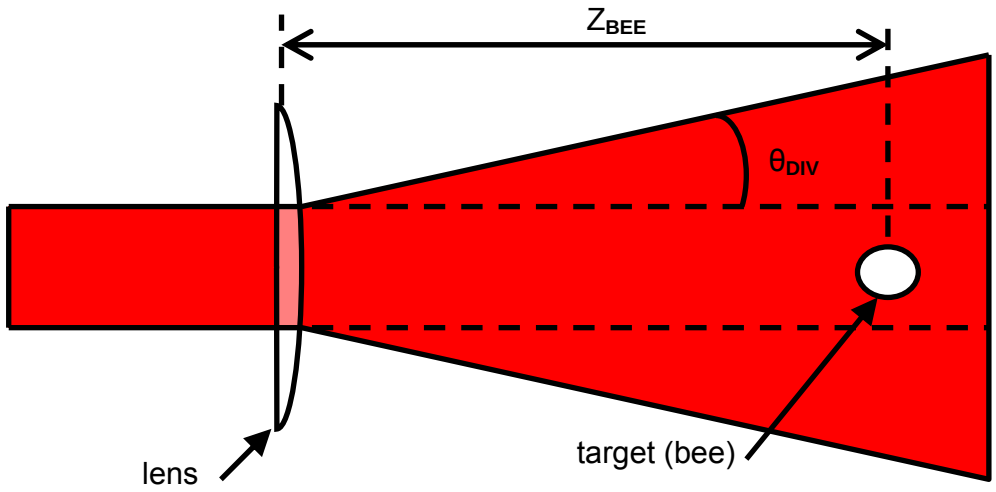

Assuming a total laser power P_0 at the transmitting lens, the irradiance leaving the WMD is as follows:

$$E_0 = \frac{P_0}{\pi r_0^2} \quad \left[\frac{W}{m^2}\right] \tag{1}$$

The irradiance at the target, assuming lossless transmission, can be found similarly:

$$E_f = \frac{P_0}{\pi\left(z_{BEE}\tan\left(\theta_{DIV}\right)+r_0\right)^2} \quad \left[\frac{W}{m^2}\right] \tag{2}$$

The power hitting the bee is found by multiplying the source irradiance by the cross-sectional area of the bee:

$$P_{BEE} = A_{BEE}E_f = \frac{\pi\left(d_{BEE}\right)^2}{4}\left(\frac{P_0}{\pi\left(z_{BEE}\tan\left(\theta_{DIV}\right)+r_0\right)^2}\right) \quad [W] \tag{3}$$

While minimizing θ_{DIV} will maximize the amount of laser power incident on the target, a relatively small beam size at the target reduces the probability that a honeybee will pass through it, reducing the probability of detection.

The next step in deriving the radiometric model for the WMD is to assemble the equation for the receiver side of the system. Figure 13 shows the graphical interpretation of the receiver model. Going back to the irradiance incident on the bee, assuming a reflectivity of R_{BEE}, the irradiance leaving the bee is defined as:

$$E_{BEE} = E_f\, R_{BEE} \quad \left[\frac{W}{m^2}\right] \tag{4}$$

While the reflectivity of a honeybee is fixed for both the body and the moving wings, we will consider R_{BEE} to be a variable with an average value as well as sinusoidal behavior near the frequencies that honeybees flap their wings:

$$R_{BEE} = \overline{R_{BEE}} + r\cos\left(\omega t\right) \tag{5}$$

Figure 13. Radiometric model of the Wingbeat Modulation Detector receiver.

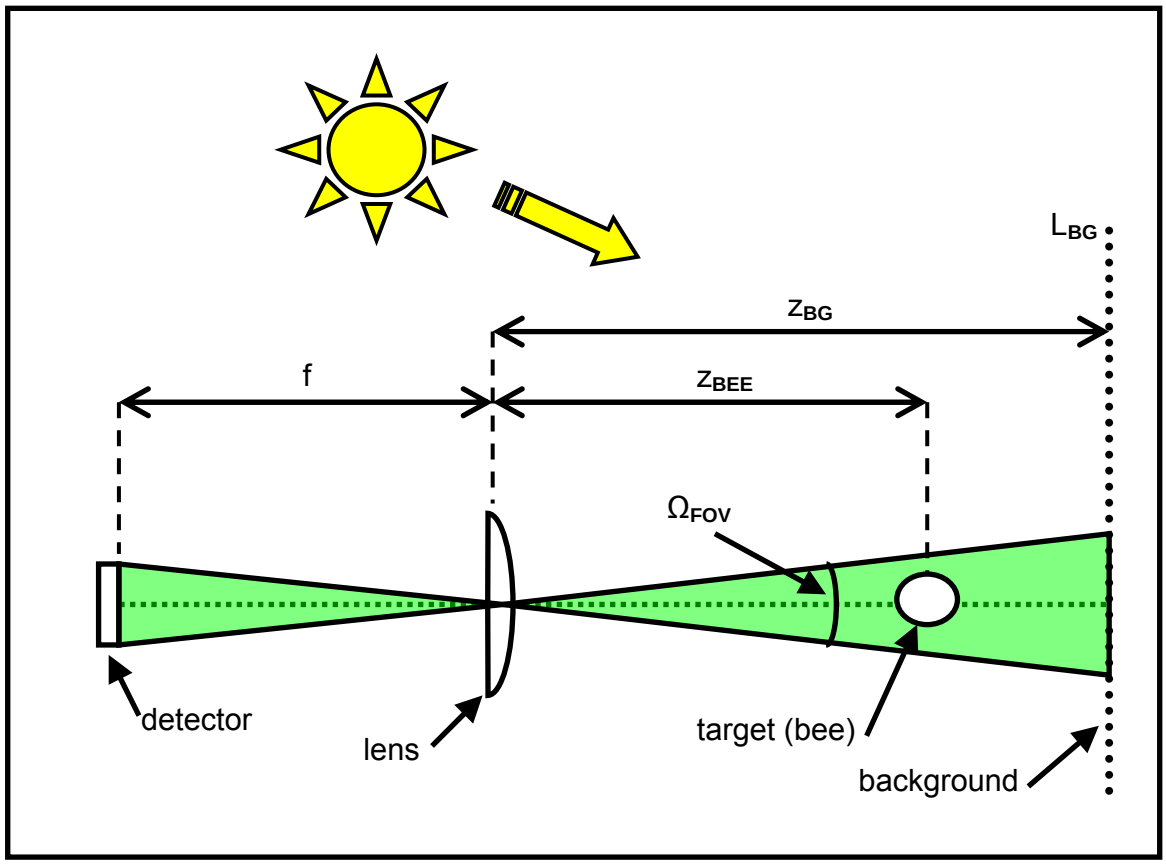

Using E_{BEE}, the irradiance at the entrance pupil can be found by taking the ratio of the projected solid angle of the entrance pupil as seen by the bee to the projected solid angle into which the bee scatters. For now, we assume that the bee scatters light into a hemisphere, which has a solid angle of π steradians. The projected solid angle of the entrance pupil as seen by the bee is given approximately by:

$$\Omega_{EP,BEE} = \frac{A_{EP}}{z_{BEE}^{\ 2}} = \frac{\pi\left(d_{EP}\right)^2}{4 z_{BEE}^{\ 2}} \quad [sr] \tag{6}$$

$$\Omega' = \frac{\Omega_{EP,BEE}}{\Omega_{SCAT}} = \frac{\left(\frac{\pi (d_{EP})^2}{4 z_{BEE}{}^2}\right)}{\pi} = \frac{(d_{EP})^2}{4 z_{BEE}{}^2} \quad \left[\frac{sr}{sr}\right] \tag{7}$$

Using Ω', we can calculate the irradiance of the backscattered light at the entrance pupil:

$$E_{EP} = \Omega' E_{BEE} \quad \left[\frac{W}{m^2}\right] \tag{8}$$

The power at the detector will be the irradiance at the entrance pupil multiplied by the glint area of the bee wing, A_{BEE} and also the transmission of the optics, τ_{OPTICS}:

$$P_{DET} = E_{EP}\, A_{BEE}\, \tau_{OPTICS} = \frac{P_0\, R_{BEE}\, (d_{EP})^2\, (d_{BEE})^2\, \tau_{OPTICS}}{16 (z_{BEE} \tan(\theta_{DIV}) + r_0)^2\, z_{BEE}{}^2} \quad [W] \tag{9}$$

In addition to modeling the power at the detector scattered by the target, the background light must also be accounted for. If the FOV of the detector is known, along with the background spectral radiance L_{BG}, the power at the detector from background light can be found with:

$$P_{BG} = A_{EP}\, \Omega_{FOV}\, \tau_{OPTICS} \int_{\lambda_1}^{\lambda_2} L_{BG}(\lambda) \tau_{BG}(\lambda) d\lambda \quad [W] \tag{10}$$

In this equation, $\tau_{BG}(\lambda)$ represents the spectral transmission of the atmosphere. To simplify this model, we will ignore the effects of atmospheric transmission and the losses in the optics; also, we will assume that the background radiance is fairly constant over the range from λ_1 to λ_2. Instead, we will define $\overline{L_{BG}}$ as the average background radiance from λ_1 to λ_2. With these two changes, the simplified model is:

$$P_{BG} = \overline{L_{BG}}\, A_{EP}\, \Omega_{FOV}\, \Delta\lambda \quad [W] \tag{11}$$

In the above equation, $\Delta\lambda$ is the spectral width of the background light entering the detector, determined by the spectral transmission of the receiver optics. For this instrument, the only optic strongly constraining $\Delta\lambda$ is the narrowband interference filter. One way of finding the far-field projected solid angle of the FOV, Ω_{FOV}, is to measure the field of view at a given distance and divide by the square of that distance. From the alignment tests, the field of view was estimated to be 0.24 m^2 at a range of 30 m, equating to a solid angle of roughly 2.67 * 10^{-4} steradians. Alternatively, Ω_{FOV} can be found be dividing the active area of the detector by the square of the distance between the detector and the primary lens. With an active detector area of 160 mm^2, and distance between the detector and the lens roughly 450 mm, the solid angle would be 7.90 * 10^{-4} steradians. Since both of these values for the solid angle are based on estimations yet fairly close to each other, we can assume the true value is at least on the order of 10^{-4} steradians.

With equations for P_{DET} and P_{BG}, we can approximate a signal to background ratio (SBR) with respect to optical power by taking the ratio of these two equations:

$$SBR_{dB} = 10\log_{10}\left(\frac{P_0\, R_{BEE}\left(d_{BEE}\right)^2}{4\pi\left(z_{BEE}\tan\left(\theta_{DIV}\right)+r_0\right)^2\left(z_{BEE}\right)^2\,\overline{L_{BG}}\,\Omega_{FOV}\,\Delta\lambda}\right) \tag{12}$$

To simplify the SBR equation, we will assume zero divergence on the laser beam and a value of 1 for R_{BEE}. The SBR equation is now as follows:

$$SBR_{dB} = 10\log_{10}\left(\frac{P_0\left(d_{BEE}\right)^2}{4\pi\left(r_0\right)^2\left(z_{BEE}\right)^2\Omega_{FOV}\left(\overline{L_{BG}}\,\Delta\lambda\right)}\right) \tag{13}$$

To find a reasonable value for $\overline{L_{BG}}$, the Moderate Resolution Transmittance Code (MODTRAN) was run using the PCMODWIN atmospheric radiative transfer program, a product of the Ontar Corporation. Using this program, atmospheric and geometric conditions that the instrument would experience are used to calculate the total atmospheric radiance that would be seen by the detector. By assuming a slightly downward-looking path of 200 m length very close to the ground, with a spectral range from 803 nm to 813 nm and a surface albedo index of -9.0 (a MODTRAN model for vegetation), the total integrated radiance reported by MODTRAN is 1.3 * 10^{-4} W/ cm^2 sr.

With values for Ω_{FOV} and $\overline{L_{BG}}$, the signal-to-background ratio can now be found. Assuming a value of 10 meters for z_{BEE}, an initial beam radius of 25 mm, 100 mW of laser power and a circular glint area on the bee wing with diameter of 2 mm, the SBR equation falls out like this:

$$SBR_{dB} = 10\log_{10}\left(\frac{(.100W)(.002m)^2}{4\pi(.025m)^2(10m)^2(8*10^{-4}sr)(1.3\,W/m^2\,sr)}\right)$$

$$SBR_{dB} = 10\log_{10}\left(4.89*10^{-4}\right) = -33.1dB$$

At first, a signal to background ratio of -33.1 dB may seem a little discouraging, yet this figure of merit may not immediately merit much of anything, as this number shows nothing more than the contrast between backscattered laser light and background radiation: detecting honey bees requires that this instrument be able to detect modulation in this backscattered laser light. However, this figure does say that without modulation of the backscattered light, this instrument would be incapable of direct detection LIDAR based on the poor contrast between laser light and background light.

While a few small factors in the SBR equation have been justifiably ignored (transmittances of the atmosphere and optics), one factor that must come back into consideration is the equation for R_{BEE}, since we have chosen the reflectivity of the bee as the variable that accounts for the modulation of the backscattered light by the honey bee. To find the sensitivity of the WMD to modulation in backscattered laser light from a honey bee, we need to put the equation for bee reflectivity back into the SBR equation and isolate the variable responsible for modulation. Rewriting the SBR equation with this in mind, we get:

$$SBR_{dB} = 10\log_{10}\left(\frac{P_0\left(\overline{R_{BEE}} + r\cos(\omega t)\right)\left(d_{BEE}\right)^2}{4\pi\left(r_0\right)^2\left(z_{BEE}\right)^2\Omega_{FOV}\left(\overline{L_{BG}}\,\Delta\lambda\right)}\right) \tag{14}$$

With a little bit of re-arranging, the above equation can be expressed as:

$$SBR_{dB} = 10\log_{10}\left(\overline{R_{BEE}} + r\cos(\omega t)\left(\frac{P_0\left(d_{BEE}\right)^2}{4\pi\left(r_0\right)^2\left(z_{BEE}\right)^2\Omega_{FOV}\left(\overline{L_{BG}}\,\Delta\lambda\right)}\right)\right) \tag{15}$$

Since we are only interested in modulated laser light, we will ignore $\overline{R_{BEE}}$ and focus on the part of the SBR equation involving $r\cos(\omega t)$:

$$SBR_{dB} = 10\log_{10}\left(\frac{r\cos(\omega t)P_0\left(d_{BEE}\right)^2}{4\pi\left(r_0\right)^2\left(z_{BEE}\right)^2\Omega_{FOV}\left(\overline{L_{BG}}\,\Delta\lambda\right)}\right) \tag{16}$$

Up to this point, no assumption has been made about r; however, we do know that R_{BEE} cannot take on a value outside of the range from 0 to 1, as R_{BEE} represents a reflectivity. From laboratory measurements of real bee wings, the reflectivity of a bee wing was found to be roughly 0.15; we will assume that this value can change by ± 10% as the wings are beating. This corresponds to minimum and maximum values of 0.145

and 0.165, respectively, which means that *r* will take on a value of 0.01 corresponding to a peak-to-peak sinusoidal value of 0.02. Using this value of *r* with the numbers from before, the SBR for the modulated light only can be found:

$$SBR_{dB} = 10\log_{10}\left(\frac{(0.02)(.100W)(.002m)^2}{4\pi(.025m)^2(10m)^2(8*10^{-4}sr)(1.3W/m^2sr)}\right)$$

$$SBR_{dB} = 10\log_{10}\left(9.79*10^{-6}\right) = -50.1dB$$

Assuming that the non-modulated component of light incident on the detector is not saturating the detector itself, the signal-to-background ratio of this instrument is -50.1 dB, and this number is based on somewhat generous assumptions. Still, this figure is not enough to give us a signal-to-noise ratio (SNR), since we need to compare the amount of energy leaving the detector at the modulation frequencies. To do this, we will multiply the amount of total light entering the detector by $\Re$, the radiant sensitivity of the PMT (units of A/W). This multiplication yields the amount of current sourced by the detector:

$$I_{DET} = P_{TOTAL}\Re \quad [A] \tag{17}$$

$$I_{DET} = (P_{DET} + P_{BG})\Re \quad [A] \tag{18}$$

$$I_{DET} = \left(1.26*10^{-9}W + 5.29*10^{-6}W\right)(0.05) = \left(2.64*10^{-7}\right) \quad [A]$$

Assuming that the detector is not limited by thermal noise, the dominant noise source will be shot noise. The root mean square (RMS) shot noise current can be found with the following equation:

$$I_{SN} = \sqrt{2q\bar{i}\Delta f} \quad [A] \tag{19}$$

In this equation, q is the charge of an electron (in Coulombs), i represents the mean current and Δf stands for the electrical bandwidth of the signal. Using I_{DET} as the mean current and 1 kHz for the electrical bandwidth (set by the filters on the preamplifier), the shot noise current can be found:

$$I_{SN} = \sqrt{2\left(1.609*10^{-19}\right)\left(2.64*10^{-7}\right)\left(1000\right)} = 9.22*10^{-12} \quad [A]$$

From above, we have the modulated power at 9.79 * 10^{-6} W; multiplying this power by the radiant sensitivity of the PMT yields a signal current of 4.90 * 10^{-7} A; this value is significantly higher than the shot noise in the detector. Dividing the signal current by the shot noise current, we obtain a SNR of 94.5 dB. Though the contrast of background light to laser light is not very good, the signal dominance over the shot noise in the detector suggests that significantly reducing the background light would allow this instrument to be operated outdoors with an acceptable SNR ratio.

Clearly, these figures suggest that the performance of the WMD outdoors should be reasonable in the current configuration. If this system were a direct detection laser system with a SBR value of -50.1 dB, it would not work. Since we are trying to detect modulation, this low SBR value is not the end of the story for this system, provided the other noise sources are smaller than the wingbeat modulation signals at the frequencies of interest. Another thing to consider is that this model has not accounted for other factors such as light leaks in the optical baffling, clipping of the laser beam in either the Tx or Rx path, etc. Still, the model for the WMD indicates that this instrument should be able to function fairly well outdoors.

CHAPTER FIVE

CONCLUSION

The Bottom Line

The theory behind the Wingbeat Modulation Detector (WMD) is sound; the results from testing the WMD using the piezoelectric polymer (PEP) indoors prove that this theory can be realized in a physical instrument. As the previous section shows, the performance of the WMD should be reasonable outdoors, but longer ranges might require modifications to increase the signal-to-noise ratio of this instrument. One thing that could be investigated is using a different wavelength laser diode: shorter wavelengths will equate to better responsivity and radiant sensitivity on the photomultiplier tube (PMT). At the same time, shorter wavelengths may result in higher levels of background radiation. Is 100 mW enough optical power to provide the necessary level of contrast against scattered solar radiance? Perhaps it is possible that we have more than enough power, and the relatively wide optical bandwidth of the interference filter and/or an unnecessarily large FOV allow too much background light to reach the detector, limiting the performance of the WMD.

Another thing that needs to be taken into consideration is the layout of the WMD; the monostatic configuration is convenient in that the field of view (FOV) and field of illumination (FOI) can stay coaxial over a long range, but as was mentioned before, the alignment process is lengthy and tedious. Also, the monostatic configuration forces the use of a polarizing beam splitter and a quarter-wave plate. Were the WMD to be

redesigned as a bistatic system, these optical components could be eliminated, and the alignment procedure would be much simpler to perform; although the alignment would change as a function of range. Another great advantage of moving to a bistatic configuration is that the use of a pre-fabricated telescope would be much simpler. In addition to having greater light gathering ability, the FOV of a telescope would likely be much narrower; this effect could help reduce the amount of background light reaching the detector. As with the other suggestions, the use of a telescope needs investigation.

Future Work

One of the largest shortcomings of the WMD is the inherent inability of this instrument to differentiate between targets modulation light at different ranges. A traditional LIDAR lacks the ability to detect modulation, but by design possesses ranging capability. It may be possible to design an instrument that has both a continuous-wave and a pulsed laser, operating at different wavelengths that would be able to detect modulation and range from backscattered light. The major problem with a two-color hybrid system like this is clearly the complexity: two lasers, two detectors and all the electronics required to run them would make for a bulky instrument.

Going back to the shortcomings of a traditional LIDAR, the reason that this pulsed-laser type system cannot be used to resolve modulation is the repetition rate of the laser itself, which is usually on the order of tens of cycles per second. Thinking in terms of sampling frequency, it should be readily apparent that data recorded from a laser pulsed at tens of Hz will not be able to resolve modulation occurring between 200 Hz and

300 Hz. This suggests that if a laser could be found with a suitable repetition rate, it may in fact be possible to resolve modulation in the backscattered light while retaining range information using only one laser. For the last year at Montana State, a team of undergraduate researchers led by Dr. Kevin Repasky, as part of a collaborative project of the Lasers and LIDAR group that includes Dr. Repasky, Dr. Joseph Shaw, Dr. John Carlsten and Dr. Lee Spangler, have been developing such a system built around a laser with a repetition rate of roughly 7 kHz. Early tests suggest that this instrument will be able to detect wingbeat modulation from a honeybee as well as resolve range information.

REFERENCES CITED

Bender, S. F. A., P. J. Rodacy, R. L. Schmitt, P. J. Hargis, Jr., M. S. Johnson, J. R. Klarkowski, G. I. Magee, and G. L. Bender, 2003, "Tracking Honey Bees Using Lidar (Light Detection and Ranging) Technology," Sandia Report SAND2003-0184, Sandia National Laboratory, Aluquerque, NM 87175.

G.W. Bohannan, V.H. Schmidt, R.J. Conant, J. Hallenberg, C. Nelson, A. Childs, C. Lukes, J. Ballensky, J. Wehri, B. Tikalsky, and E. McKenzie, 2000, "Piezoelectric polymer actuators in a vibration isolation application," *Proc. SPIE Smart Structures and Materials*, Vol. 3987, 331.

Bromenshenk, J. J., C. B. Henderson, and G. C. Smith, 2003: "Biological Systems, paper II," in "Alternatives for landmine detection" (RAND Corp.)

Bromenshenk, J.J., C. B. Henderson, Robert A. Seccomb, Steven D. Rice, Robert T. Etter, S. F. A. Bender, Phillip J. Rodacy, Joseph A. Shaw, Nathan L. Seldomridge, Lee H. Spangler and James J. Wilson, 2003: "Can Honey Bees Assist in Area Reduction and Landmine Detection," *J. Mine Action*, 7.3.

Chadwick, L. E., 1939: "A simple stroboscopic method for the study of insect flight," *Psyche*, 46: 1-8.

MacDonald, J. , J. R. Lockwood, J. McFee, T. Altshuler, T. Broach, L. Carin, R. Harmon, C. Rappaport, W. Scott Weaver, 2003: "Alternatives for landmine detection" (RAND Corp.)

Moore, A., J. R. Miller, B. E. Tabashnik, and S. H. Gage, 1986: "Automated identification of flying insects by analysis of wingbeat frequencies," *J. Econ. Entomol.*, 79: 1703-1706.

Phelan, James M., James L. Barnett, 2002: "Chemical Sensing Thresholds for Mine Detection Dogs," *Proc. SPIE*, 4742: 532-543.

Reed, S. C., C. M. Williams, and L. E. Chadwick, 1942: "Frequency of wing-beat as a character for separating species races and geographic varieties of Drosophila," *Genetics*, 27: 349-361.

Richards, I. R., 1955: "Photoelectric Cell Observations of Insects in Flight," *Nature*, 175: 128-129.

Shaw, Joseph A., Nathan L. Seldomridge, Dustin L. Dunkle, Paul W. Nugent, Lee H. Spangler, Jerry J. Bromenshenk, Colin B. Henderson, James H. Churnside, James J. Wilson, 2005: "Polarization lidar measurements of honey bees in flight for locating landmines", *Optics Express*, 13, 15: 5853-5863.

Unwin, D. M., and C. P. Ellington, 1979: "An optical tachometer for measurement of the wing-beat frequency of free-flying insects," *J. Exp. Biol.*, 82: 377-378.